TECHNICAL ARTICLE

About the irradiance and apertures of camera lenses

by Dr. Vladan Blahnik, Carl Zeiss AG

July 2014

Introduction

Lens aperture is responsible for the degree of irradiance striking the image plane, which – in addition to film or image sensor sensitivity – determines the brightness of the image. While in photography low lighting can be compensated with longer exposure times, in cine film with its stipulated image rate of usually 24 frames per second exposure is typically controlled by lens aperture. For this reason, lenses with large apertures are much sought after especially by professional cinematographers.

As early as 1927, Willy Merté at ZEISS in Jena calculated a series of fast movie lenses with an aperture of f/1.4. These lenses were available with focal lengths of 20 and 25mm for 16mm-cine cameras and with the focal lengths 40, 50 und 70mm for 35mm motion picture cameras (format 18mm x 24mm).

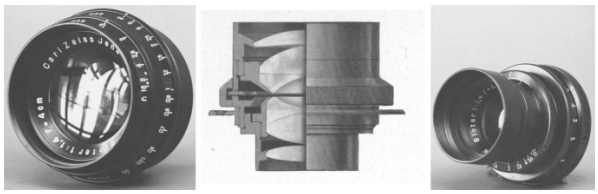

Fig. 1: Left: Biotar f/1.4, f=40mm for 35mm film; center: Biotar lens design drawing; right: Biotar f/1.4, f=25mm for 16mm film.

As compared to the formerly utilized lenses with apertures of f/6.3 or f/5.6 this corresponds to a relative increase in the maximum irradiance by a factor of approximately 20. This high luminosity makes it possible to take images in low ambient light, such as in candle-lit rooms. For his 1975 film “Barry Lyndon“, Stanley Kubrick specifically requested a Planar 0.7/50mm from Carl Zeiss to be able to capture the authentic candlelight atmosphere in the castle without additional lighting. This lens was originally developed for NASA for images to be taken on the back side of the moon.

Fig. 2: Image taken with the Planar 0.7/50mm.

The concept of the ”f-stop” or “f-number” of a lens is ridden with confusion and erroneous information, as was described by Douglas S. Goodman in his article “The F-word in Optics.” And yet it is not difficult to define the aperture – without approximations – in a manner such that it will characterize the irradiance of a camera lens for any given object distance. We will provide an overview of the functional dependence of the aperture from the distance to the object by means of a few lens data and discuss the underlying mechanisms. In this discussion, only the irradiance in the center of the image field will be discussed. The functional dependency of the irradiance at the edge of the image field requires taking into account light beam limiting field stops (vignetting) and various cosine factors to describe oblique light incidence and/or emission. This was exhaustively researched by Ernst Wandersleb (1952).

High performance optics as a black box: Ernst Abbe's sine condition

Regardless of how complex and multifaceted these optical designs can be, every camera lens can be described as a "black box" following the same rules: For an object point in the center of the image, the object and image side angles of the same ray fulfill the Abbe sine condition. The clipping of the light cone from this object point is defined by the entrance and exit pupil (i.e. by the image of the iris diaphragm forward or backward through the system respectively).

The Abbe sine condition states that when a lens is properly corrected on the optical axis, the sine of the angle between a ray and the optical axis must be proportional to the sine of the corresponding ray angle in the image space, i.e.

$$\beta \sin \vartheta' = \sin \vartheta,$$

so that the lens will also be properly corrected for the light emanating from object plane, perpendicular to the optical axis, in a (local) extended area in the image plane. The proportionality constant β is the magnification, i.e. the ratio of the image size to the object size. Although Abbe had first formulated this condition for the imaging theory of microscopes (Abbe (1873)), it is also met in modern camera and cine lenses even at maximum aperture (where usually a certain amount of spherical aberration is permissible) to a very good degree of approximation. Abbe used the term "aplanatic" for lenses that fulfill the sine condition (for a detailed explanation cf. Abbe (1879)).

The sine condition can be derived from Fermat's principle, according to which two points in space (in this case, the object point P and the image point P′), are joined by a light ray whose optical path length (the product of the refractive index and the path length) is shorter than that of any other adjacent path.

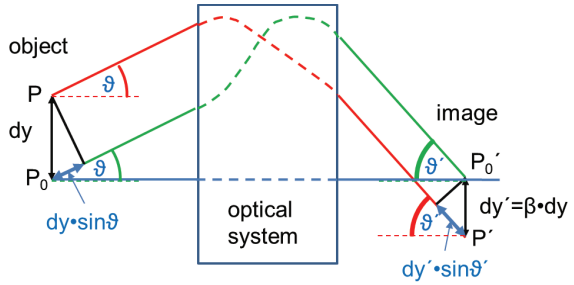

Fig. 3: On Abbe´s sine condition.

The derivation of the sine condition can be briefly sketched as follows:

For good optical correction, all rays shown in the drawing (fig. 3) must have the same optical path length; this applies to the removal of spherical aberration on the axis (cf. the blue and green rays) as well as to the ray emanating from a closely neighboring object point on the vertical plane under the same angle ϑ, which – because we are considering a very small range of the field – both strike the image plane at (almost) the same angle ϑ′. The optical paths of the two non-axial rays (red and green) are equal in length only when the path dy·sinϑ is equal to the distance dy′·sinϑ′. As dy′/dy = β is the magnification, this results in β·sinϑ′=sinϑ. Detailed proofs in various different variants can be found in Czapski (1904), p. 123-132, Conrady (1905) and in many physics textbooks (e.g. Schmutzer (1989) or Weizel (1949)).

The following simple example will show what happens when the sine condition is violated. For this purpose we shall examine two different single lenses, a hyperboloid lens and an aplanatic lens, imaging a small area around the optical axis of an infinitely distant object plane.

Hyperboloid Lens

It is possible to obtain a perfect image of an infinitely distant object point with a single lens if its front surface is planar and its rear surface

is hyperbolic (Kingslake (1978), p. 113). However, as will be seen only the axial image is perfect and the off-axis image is afflicted by significant aberrations.

Aplanatic Lens

If, on the other hand, the lens is optimized at a high aperture for an extended object range, surfaces with a curvature directed away from the image element will result. To correct for the spherical aberration, the surfaces are aspherically curved (i.e. they do not have a spherical form).

The lenses are shown in fig. 4 drawn to the same scale: They have the same image-side aperture angle of 49° (corresponding to NA´ = sin(49°) = 0.75) and the same (axial) focal length. As can be seen in fig. 4 the lens diameter of the aplanatic lens is much smaller. The point spread functions on the optical axis (0°) and those for objects reaching the lens from a slightly oblique angle (0.1° und 0.2°) are shown on the right.

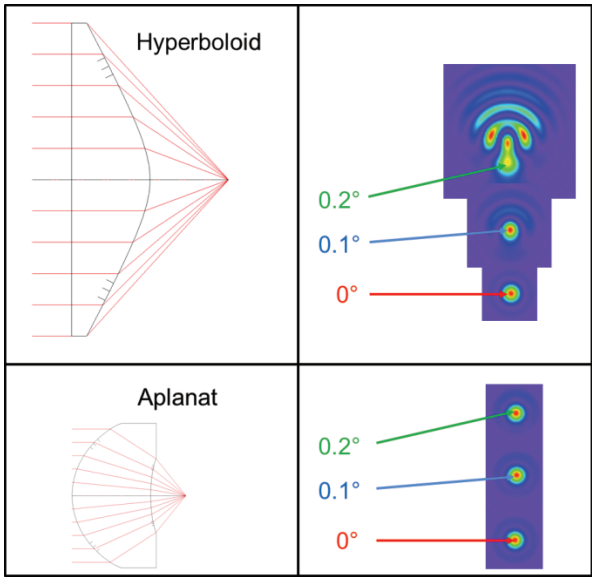

Fig. 4: Hyperbolic and aplanatic single lens (shown on same scale) and their point spread function for imaging near the optical axis.

If the respective sizes of the two lenses are scaled in a manner such that their focal lengths are f = 1mm in each case, then in fig. 4 the point spread functions and the distances between them are represented to scale (with this focal length, an object angle of 0.1° corresponds to a distance of approximately 1.7µm in the image plane). The aberration that occurs predominantly when the sine condition is violated is coma. This can be recognized in the figure by the fact that the upper point spread function has the shape of the tail of a comet.

In microscopy or optical lithography, the maximum angular aperture of the light cone is characterized by means of its numerical aperture (abbreviated NA). It is defined on the image side as the sine of the maximum angle under which light reaches the image point times the refractive index of the medium in the image space:

$$NA' = n' \sin \vartheta'_{\max}.$$

In photography, the refractive index n´ always refers to air, i.e. n´=1. In current optical lithography systems with an exposure wavelength of 193nm, an immersion liquid (water between the last lens and the image plane) is used in order to increase further the numerical aperture, e.g. to NA´=1.35, so that even smaller structures can be exposed.

The angle of the edge of the cone in the object and image space is defined by the position and size of the entrance and exit pupil respectively. When looking against a bright background from the object space into a lens, one can see the entrance pupil of the lens as a bright, circular disc. Stopping down the lens, it can be seen how the disc becomes smaller, with a diameter inversely proportional to the f-number engraved on the aperture ring. Usually, the shape of the entrance pupil will change somewhat: It becomes angular corresponding to the number of diaphragm blades (fig. 5). The position of the entrance pupil is the image of the iris diaphragm (which in camera lenses is almost always virtual) – or, more accurately, of the smallest limiting stop in the lens, which is im-

aged by the lens elements positioned in front of it towards the object space. Accordingly, what one sees is the exit pupil when looking into the lens from the image side.

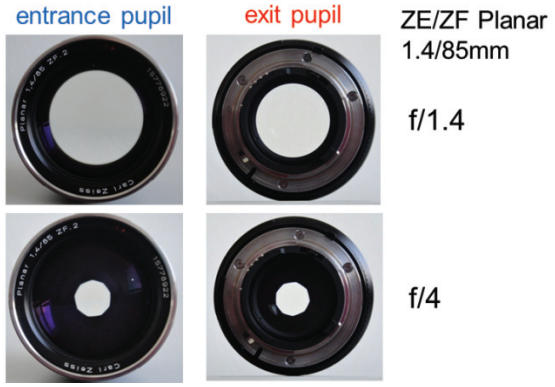

Fig. 5: Entrance and exit pupil of the ZE/ZF Planar 1.4/85mm at maximum aperture f/1.4 and stopped down f/4.

If $\varnothing_{AP}$ defines the diameter of the exit pupil measured as (twice the) distance from the optical axis to the edge of the exit pupil, the numerical aperture can also be written as the quotient of the exit pupil height to the distance of the exit pupil to the image plane:

$$NA' = n' \frac{Ø_{AP}}{2\,s'}.$$

The exit pupil diameter $\varnothing_{AP}$ refers to the circular opening cut out of the exit pupil sphere. The position of this circular disc changes slightly when stopping down, as the entrance and exit pupils are spherical.

In the following schematic illustration (fig. 6), the entrance and exit pupils are drawn as having the same size. Generally, their sizes may differ, but the entrance pupil heights (measured in the plane that is axially perpendicular to the optical axis) are transferred on a linear basis to the exit pupils with the pupil magnification

$$\beta_p = \frac{Ø_{AP}}{Ø_{EP}}.$$

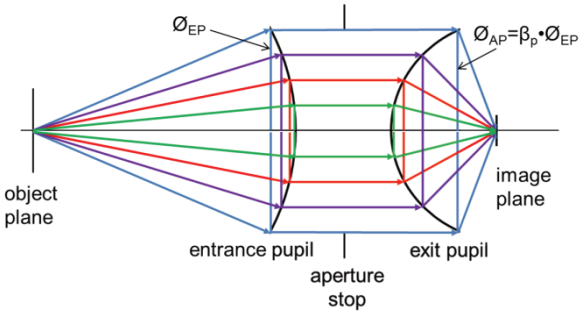

Fig. 6: The entrance and exit pupil of an optical system described as „black box“ (pupil magnification β_p=1 assumed).

From the sine condition it follows, firstly, that the relationship between numerical object and image side aperture is given by NA=β·NA´.

Secondly $$\beta = \frac{\sin\vartheta}{\sin\vartheta'} = \frac{Ø_{EP}/2s}{Ø_{AP}/2s'} = \frac{s'}{\beta_p\, s},$$

whence:

$$\frac{s'}{s} = \beta_p\,\beta.$$

In a graphic representation, this means that one can imagine the object point and the image point surrounded by spheres whose radial ratio is the product of the magnification β and the pupil magnification β_p. The heights of the intersection points of the entering rays with the entrance pupil sphere are then equal to those of the exiting rays with the exit pupil sphere (in figs. 6 and 7, β_p=1 has been chosen).

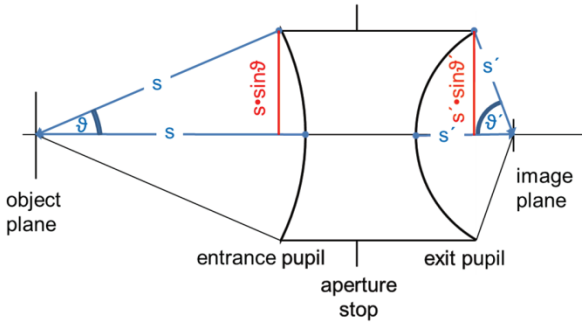

Fig. 7: Lens as “black box.”

Therefore, in an aplanatic lens the entrance and exit pupils are spherical surfaces and not planes. This confusion is the reason why in some representations the tangent instead of the sine is erroneously stated in connection with the definition of the aperture number. However, in the ratio of pupil size to pupil distance, the distances s and s´ are hypotenuses and not catheti.

Focusing of a lens with focal length f´ characterized by means of the entrance pupil and the exit pupil is described by the following paraxial imaging equation (the refractive index in the object and image space is assumed to be equal to 1):

$$-\frac{1}{\beta_p s}+\frac{\beta_p}{s'}=\frac{1}{f'}$$

Max Berek derived this relation in 1930 in his textbook "*Grundlagen der praktischen Optik*" ["Principles of Practical Optics"]. Unfortunately, this equation seems to have fallen into oblivion in many modern optics texts. This probably explains why sometimes conclusions are drawn that in fact apply only to symmetrical lenses:

The pupil magnification β_p is equal to one only for lenses that are strictly symmetrical about the aperture. However, most telephoto and retrofocus lenses do not have such a symmetric design.

By introducing $\frac{s'}{s}=\beta_p\,\beta$ in this paraxial focus condition and eliminating the object distance s, we obtain the distance between the exit pupil and the image plane:

$$s'=\left(\beta_p-\beta\right)f'.$$

As the entrance and exit pupils are images of the iris diaphragm, their position in the lens can be determined directly from the schematic lens diagram when an off-axis chief ray is included (fig. 8): The position of the entrance pupil in a lens lies at the intersection of the optical axis with the extension of the chief ray of an off-axis object point. The chief ray by definition crosses the optical axis at the position of the stop. Similarly the position of the exit pupil results from the intersection of (the extension of) this chief ray with the optical axis. The following illustration fig. 8 shows the ZE/ZF Planar 1.4/85mm and the ZE/ZF Distagon 2.8/21mm including their entrance and exit pupils. The abbreviations EP for entrance pupil (german: "Eintrittspupille")) and AP for exit pupil (german: "Austrittspupille")) are used.

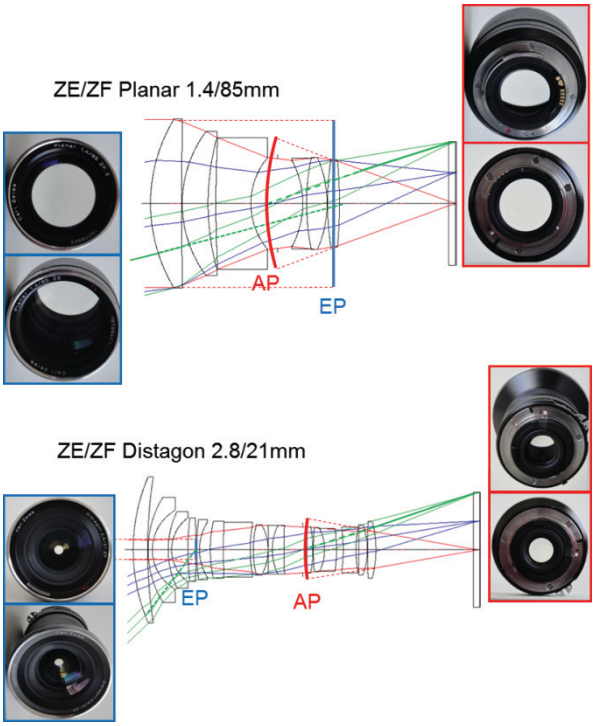

Fig. 8: Entrance and exit pupil at center and corner of field of the ZE/ZF Planar 1.4/85mm and ZE/ZF Distagon 2.8/21mm.

While the irradiance only depends on the angular aperture, the pupil position has an effect on the perspective of the image. The entrance pupil position should be the pivot point for camera panning for natural perspective imaging, as it is the perspective center of a lens. This means that objects situated behind one another remain in the same arrangement

when the camera pans about the entrance pupil (fig. 9).

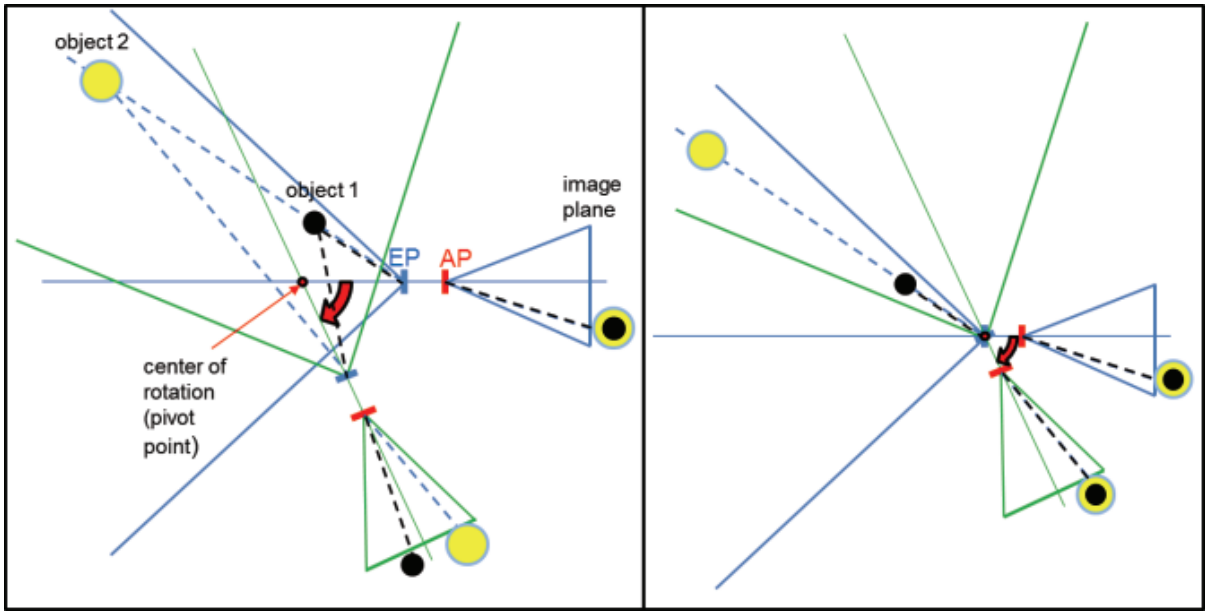

Fig. 9.: In the original view (blue field of view) the black object lies directly in front of the yellow one. If the camera is panned around a point that is different from the entrance pupil, the yellow object is shifted sideways with respect to the black one in the new field of view of the camera (green rays). When panning about the entrance pupil, the black object remains directly in front of the yellow one: There is no parallax.

F-number

Whereas the numerical aperture is used in microscopy or photolithography, in photography the light cone which converges to the image point is characterized by the f-number, here referred to as K (in the literature, often F# or f#). The f-number or f-stop is defined as half the reciprocal value of the numerical aperture (assuming a refractive index of n´=1 in the image space):

$$K = \frac{1}{2\,NA'} = \frac{1}{2\sin\vartheta'_{\max}}.$$

This equation refers to the image space light cone where NA´ is the image side (denoted primed) numerical aperture and $\vartheta'_{\max}$ is the contact angle of the aperture cone. The relative aperture is the reciprocal f-number. The notation takes the form f/K or 1:K, thus e.g. for a lens with an aperture value of K=2.8 the relative aperture or simply “aperture” (e. g. Kingslake (1989)) is f/2.8 or 1:2.8. As the sine function is never greater than 1, the aperture cannot have a value less than 0.5.

The functional dependence of the f-number on lens magnification β is described by the following relationship: $K = \left(1 - \frac{\beta}{\beta_p}\right)\frac{f'}{\varnothing_{EP}}$.

This relationship follows the equation set given earlier in the text (“S. C.“ = sine condition):

$$K = \frac{1}{2\,NA'} \overset{S.C.}{=} \frac{\beta}{2\,NA} = \frac{\beta}{\frac{\varnothing_{EP}}{s}} = \frac{s'}{\beta_p \varnothing_{EP}}$$

$$= \frac{(\beta_p - \beta) f'}{\beta_p \varnothing_{EP}} = \left(1 - \frac{\beta}{\beta_p}\right)\frac{f'}{\varnothing_{EP}}$$

The pupil magnification β_p is “forgotten” even in some highly renowned textbooks on optics.

And yet, in the closer distance range, and depending on the structure of the optical system, there are substantial differences in the functional dependence of the aperture versus magnification or object-to-image-distance, especially as a result of the deviation from the value = 1, as would be the case with a lens that would be symmetrical about the diaphragm.

If the object is in the infinity range (magnification β=0), the f-number or aperture is the quotient of the lens focal length and the diameter of the lens' entrance pupil.

$$K_0 = \left.\frac{f'}{Ø_{EP}}\right|_{\beta=0} .$$

For the magnification β=0, i.e. an infinite object distance, this aperture was characterized with the index "0". This is the "initial aperture" which is used as standard parameter to characterize "lens speed."

The entrance pupil diameter $Ø_{EP}$ and the focal length f′ can be directly read off from the representation of the ray pathway of a lens with an infinite object distance (cf. fig. 10). The focal length f′ is the distance from the pertinent intersection points of the rays striking the lens in parallel from infinity with the pertinent backward extended, image side aperture rays to the image plane. In paraxial optics the surface of all these intersecting principal points is called principal plane. For a real, that is aplanatic, lens this principal surface is in fact a hemisphere.

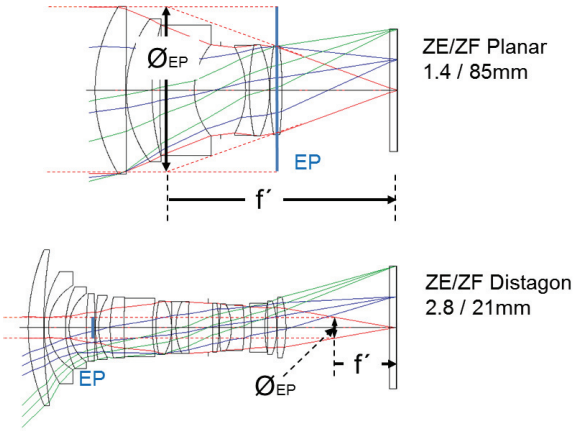

Fig. 10: Focal length f′ and entrance pupil diameter $Ø_{EP}$ of the ZE/ZF Planar 1.4/85mm and the ZE/ZF Distagon 2.8/21mm.

The "#" in the designation for the relative aperture "f/#" therefore means "diameter of the entrance pupil, when the lens is focused on infinity".

That Abbe's sine condition is necessary for the equation $K_0=f'/∅_{EP}$ to hold becomes apparent if we briefly return to our example of the single "hyperboloid" and "aplanatic" lenses:

According to fig. 11 for the aplanatic lens, the values of f′/(2h) (where h is the pupil height) and 1/(2sinϑ′) are equal in size over the entire pupil range. The f-number for maximum lens aperture (here $ϑ'_{max}$=49°, that is NA′=0.75) for the aplanatic lens is $K=1/(2\sin ϑ'_{max})$=0.67. For the hyperboloid lens, in contrast, at maximum aperture the value is much smaller: f′/(2h)= $f'/∅_{EP}$ ≈0.25. This is one half of the smallest theoretically achievable value of the f-number K according to the definition K=1/(2NA′).

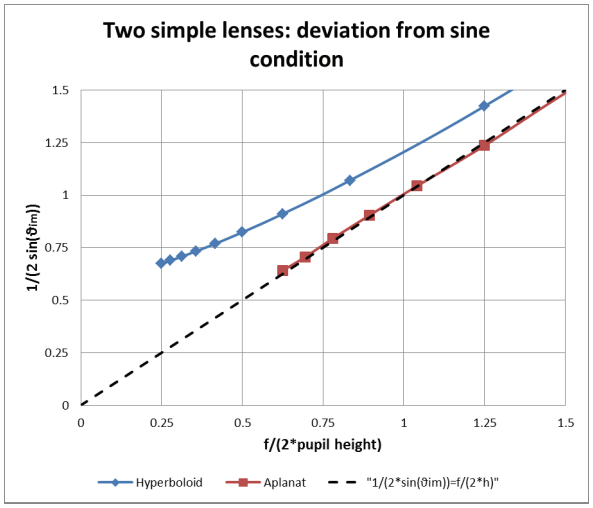

Fig. 11: The data of the simple lenses show that for the aplanatic lens sin ϑ'=h/f′ (and particularly 1/(2NA′)= f′/$\varnothing_{EP}$) holds. The hyperbolic lens significantly deviates from this relation.

Geometrically the equation sinϑ'=h/f′ simply means that the rear principal surface of the lens is of spherical shape, centered at the image point (cf. fig. 12). This is the case with the aplanatic lens. With the hyperboloid lens, however, the distances from the principal points to the image point distinctly increase towards the edge of the pupil. In this case they are located directly on the rear hyperbolic surface of the lens.

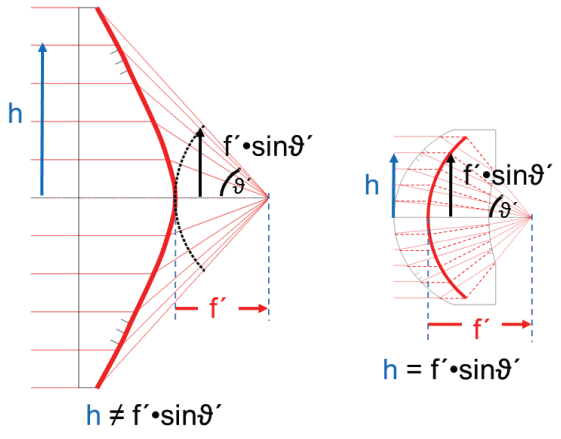

Fig. 12: Rear principal surface of aplanatic lens (sphere) and hyperboloid lens (hyperbolic shape).

Irradiance

We shall now examine the irradiance in the image plane, which we denote E′: This is the radiant power impinging on the image plane per unit area; it is measured by means of the physical unit W/m². It depends on how much light arrives from a surface element to the lens (and thus onto the image plane) and on the size ratio the surface element is imaged in the image plane.

This leads us to the connection between irradiance and lens parameters:

1. a) The radiant power arriving from a (small) surface element of an object at a distance s to the entrance pupil of the lens is obviously proportional to the area of the entrance pupil:

$$E \sim \varnothing_{EP}^2.$$

b) The strength of a spherical wave traversing an area element of a fixed size, (in this case the entrance pupil), decreases with the square of the distance.

$$E \sim \frac{1}{s^2}.$$

Therefore, we obtain the following expression for the radiant power entering the lens from a radiating surface element:

$$E \sim \frac{\varnothing_{EP}^2}{s^2} = NA^2.$$

In other words: the power of light entering the lens is proportional to the solid angle Ω, defined by the ratio of the area of the entrance pupil to the square of the object distance to the entrance pupil, i.e. $\Omega = \pi\ \varnothing_{EP}^2/s^2$. When the object distance is doubled, only a quarter of the power of light falls into the lens (cf. fig. 13).

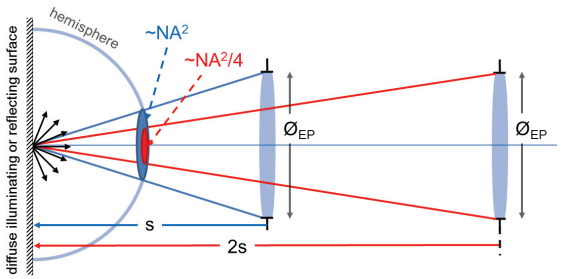

Fig. 13: On the radiant power entering the lens.

2. The irradiance in the image plane also depends on the magnification with which the object-side surface element is transferred into the image plane.

The larger the image area dF′ onto which the beam emitted by the object-side surface element dF is distributed, the smaller the irradiance in the image plane (cf. fig. 14). Since dF′/dF is equal to the square of the magnification β, we have

$$\frac{E'}{E} = \frac{1}{\beta^2}.$$

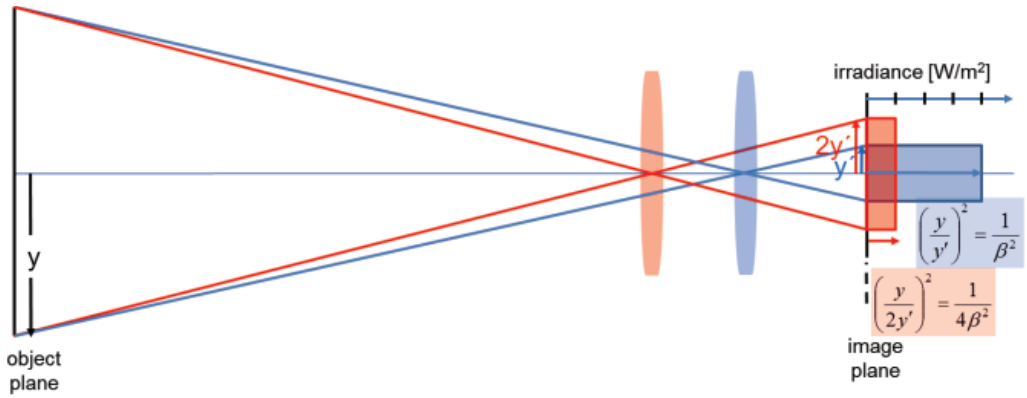

Fig. 14: Illustration with one lens for two magnifications.

Thus, with the sine condition, the following results for the irradiance in the image plane:

$$E' \sim \frac{NA^2}{\beta^2} \overset{S.C.}{=} NA'^2$$

or, expressed in terms of the f-number :

$$E' \sim \frac{1}{K^2}\ [\mathrm{W/m^2}].$$

A consequence of this relation is that a surface with uniform radiation will appear equally bright in the image plane of the lens, regardless of how far one removes oneself from it: Assuming that the distance to the lens is doubled, then, although from each object point only one-fourth of the light will reach the lens, (or, put differently, when contemplated from the object point, the solid angle under which the lens appears will become smaller by a factor of 4), the object area will be larger by a factor of 4 given twice the distance, so that the irradiance remains equal (cf. fig. 15).

The fact that the product of field and pupil remains constant is simply the result of the fact that the object field taken by the lens also remains constant. Rewriting the product yields:

$$NA \cdot y = \frac{Ø_{EP}}{s} \cdot y = Ø_{EP} \cdot \frac{y}{s} = Ø_{EP} \cdot \tan(w),$$

where w is the field-of-view angle under which the light enters the lens. For an image taken with an infinity setting, this object field is given by

$$\tan(w) = \frac{y'}{f'}.$$

This holds under the condition that the image side numerical aperture (or f-number) of the lens remains equal for both object distances. Because of

$$NA' \cdot y' = \frac{y'}{2K} = Ø_{EP} \cdot \tan(w)$$

there is a close connection between the "ramping" of the f-number and the "breathing" of the object angle. Lenses in which the f-number varies with the distance from the object tend to more significant breathing. However, this relationship is not strict: Firstly, with a fixed image height a change in aperture is also explicitly dependent on the change in the size of the entrance pupil, and, secondly, breathing depends not only on the change of the object field angle but also on the position of the entrance pupil. It can be shown that in lenses in which focusing takes place by means of movable lens groups behind the aperture diaphragm, i.e. with an entrance pupil position that remains equal when focusing, at the distance pertaining to the magnification β the object section changes in accordance with $y/y_0=1-\beta/\beta_p$. Below we shall see that in many lenses the aperture change also primarily depends on $1-\beta/\beta_p$.

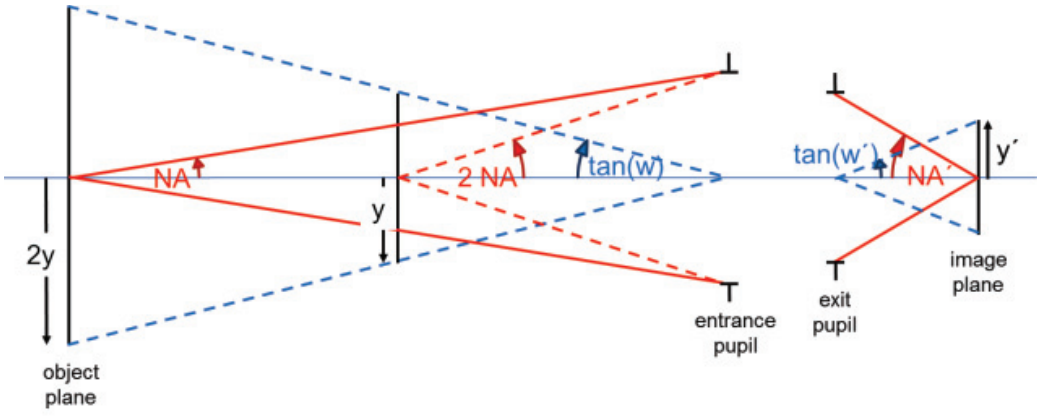

Fig. 15: On the conservation of „étendue".

This constancy of the product "Field x Aperture" applies not only to the object space, but also to the image space: this is guaranteed by the sine condition, for $NA=\beta \cdot NA'$ results in $y \cdot NA = y' \cdot NA'$ or $y^2 \cdot NA^2 = y'^2 \cdot NA'^2$. In optics, this product of field and aperture is called "étendue", "throughput" or "AΩ-product" (with the denomination A for the area and the solid angle $\Omega = \pi \cdot NA^2$). Strictly speaking, all this only applies to homogeneous and directionally constant emitting light sources and similarly transmitting optical systems, but it is frequently possible to use these parameters to approximately estimate e.g. radiation loads in illumination optics. For more accurate calculations, it is necessary to use the formulation of the conservation of the étendue in differential form and then integrate it over the beam directions and spatial distributions. These radiation conservation principles were probably first stated by Rudolf Clausius in 1864, who became famous for his formulation of the laws of thermodynamics (Chapter "On the concentration of rays of heat and light, and on the limits of its action" in his work "The Mechanical Theory of Heat": "Relationship between the enlargement and the ratio of the apertures of an elementary pencil of rays").

At first sight it may seem amazing that accordingly the irradiance of a mobile phone camera with an entrance pupil diameter of only approximately two millimeters is equal to that of a lens with same f-number of a 35mm-format camera. However, the following must be taken into account when cross-comparing lenses with different focal lengths: Although with the same f-number and the same equivalent focal length, i.e. the same maximum object angle $\tan(w_{max})=y'_{max}/f'$ that reaches the edge of the image field, the irradiance in the image plane is equal in terms of Watt/m², but with a small lens the image information is distributed over a proportionally smaller area: In a small lens, the power of light per pixel (always assuming the same number of pixels in each case), i.e. "Watt/pixel" is smaller in proportion to the area of the image field. When as a result of a smaller pixel size less light falls onto a pixel, the sensitivity for noise increases.

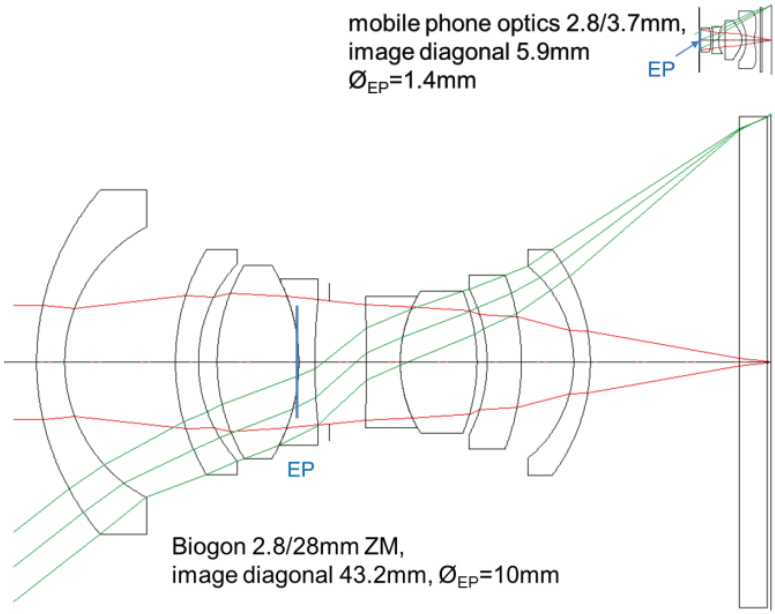

Fig. 16: Comparison of the ZM Biogon 2.8/28mm for 35 mm film format (image diagonal 43.2mm) with a mobile phone lens 2.8/3.7mm (image diagonal 5.9mm): The maximum object angles of both lenses are approximately equal at w=38° (half diagonal). They therefore have the same equivalent focal lengths. As the aperture is identical, the irradiance as radiant power per area is the same, but with the Biogon each pixel receives stronger irradiation by a factor of (43.2mm/5.9mm)²≈50.

The square function dependency of the irradiance on the aperture is the reason why the aperture steps are engraved on the diaphragm ring in multiples of $\sqrt{2}=1.4\ldots$– stopping down by one exposure step or "one stop" (e.g. from 2 to 2.8) results in a decrease of irradiance in the image plane by a factor of 2.

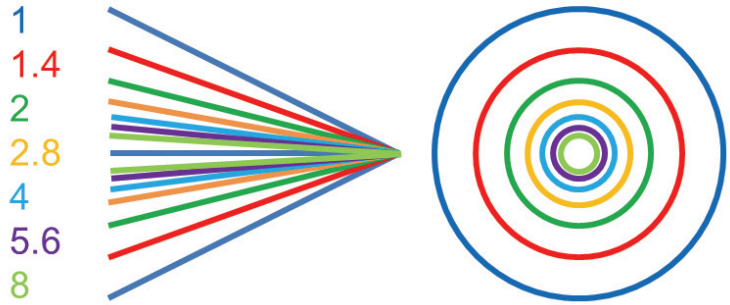

relative aperture K	numerical aperture NA´=1/(2K)	semi-aperture angle [°]	relative irradiance E´
1	0.50	30	1
1.4	0.35	20.7	1/2
2	0.25	14.5	1/4
2.8	0.18	10.2	1/8
4	0.13	7.2	1/16
5.6	0.09	5.1	1/32
8	0.06	3.6	1/64
11	0.04	2.5	1/128
16	0.03	1.8	1/256
22	0.02	1.3	1/512

Fig. 17: The standard f-number scale.

In addition, there are transmission losses in the lens due to reflection at boundary surfaces and volume absorption in the glass. With anti-reflection coatings, it is possible to achieve a reflectivity of less than 0.5% per surface in the visible spectrum, so that in a lens with 20 refractive surfaces in total less than 10% transmission is lost ($T=100\%\cdot(1-(1-R)^{\#surfaces}) = 100\%\cdot(1-(1-R)^{20})$). If the lenses were not coated, the losses would amount to as much as approximately 4-8% on one single surface. The refractive index of most types of glass lies in the range of approximately n = 1.5...1.8. The formula $R=\left(\frac{n-1}{n+1}\right)^2$ applies to reflectivity with perpendicular light incidence. In total, the transmission losses would then amount to approximately 55% to 80%.

In 1935, Alexander Smakula at Carl Zeiss in Jena, introduced a method for vacuum vapor deposition of a low refractive index layer of a thickness of only about a tenth of one micrometer onto the optical surface. This made it possible to produce clean and scratch resistant coatings quickly. At the time, they were termed "transparency optics" or "T optics" for short. Over the years, the quality of the coatings was further improved by means of multiple layers, which have been used in camera lenses under the name of Carl Zeiss T*-Coating since 1972.

As the light intensity in cinematography is set with particular precision, the lens transmission T (maximum value 1 when there are no transmission losses) is factored into the relative lens aperture, and is then called "T-Stop", "T-#" or "effective stop":

$$"\mathrm{T\text{-}stop}" = \frac{K}{\sqrt{T}}.$$

This definition takes into account that the irradiance is directly proportional to lens transmission:

$$E' \sim \frac{T}{K^2}.$$

Anti-reflection coatings are primarily used in order to prevent multiply reflected light from entering the image plane. The light from bright areas is distributed via reflections off the lenses over the entire image, and dark structures are rendered brighter, so that the image becomes pale and milky. This reduces contrast, which is particularly disturbing with coarse-grained structures. "Ghost images" and flare spots due to bright light sources can completely ruin a picture.

Fig. 18 shows images, taken for the sake of comparison with the same camera under the same exposure settings of a Planar 2.8/80mm for 6x6 medium format (uncoated for experimental purposes) (fig. 18 left column) and a Planar T* 2.8/80mm Carl Zeiss CFE for Has-

selblad with a T*-Coating (fig. 18 right column).

Fig. 18: Left column: Pictures with an uncoated Planar 2.8/80mm; right column: pictures with T*-coated Planar T* 2.8/80mm CFE.

This Planar 2.8/80mm consists of five lenses in four groups, and therefore has only eight lens surfaces in contact with air. Modern zoom optical systems, on the other hand, have multiple refractive surfaces. The Carl Zeiss Lightweight Zoom LWZ.2 T2.6/15.5-45mm has 36 surfaces, not counting cemented surfaces. The pictures shown in fig. 18 demonstrate the fundamental necessity of good anti-reflection coatings for image quality.

The dependency of the f-number on the object distance

Interestingly, the term “working aperture“ or “working f-number“ is used differently in many optics textbooks as compared to practical photography: In practice, this is simply the aperture $K_0=f'/\varnothing_{EP}$ set on the camera or lens, with which the photographs are actually taken. In SLRs, this term is used to distinguish the aperture with which the object is regarded in the viewfinder (often fully opened for a bright viewer image), from the aperture set or automatically determined for actually taking the image. In many SLR cameras there is a depth of field preview button with which the sharpness of the depth of field can be assessed to the detriment of the brightness of the image in the viewfinder.

In some optics books (e.g. Smith (2008)) in contrast, the term “working f-number” is used for the numerical aperture of lenses focusing on finite object distances.

In distance ranges that are normal in photography, with a magnification from zero to approximately -1:10, aperture changes usually lie below the perception threshold for brightness differences of approximately one third of an aperture stop.

Larger aperture changes can occur in macro lenses used for close-ups. For example, in the

ARRI/ZEISS Master Macro T2/100mm the T-stop rises from T=2 at larger object to image distance to T=4.3 in the close-up range with a magnification of -1:1. The exposure in the closer ranges must therefore be adjusted by +2.3 aperture steps as compared to the initial aperture.

Fig. 19: Exposure compensation of the ARRI/ZEISS Master Macro T2/100mm required for extreme close-ups.

In zoom lenses designed for photography, in particular in those with a longer focal length, variation in the f-number with focal length are quite typical. For instance it is not unusual that in a 70-210mm zoom lens for consumer cameras the f-number increases from 2.8 to 5.6 or more when the focal length is changed from f=70mm to 210mm. That is in the telephoto range the lens is two or more aperture stops dimmer. Since for these lens types the diameter of the front lens is usually about as large as the entrance pupil, in our example $\varnothing_{EP} = f'/K_0$ = 210mm/2.8 = 75mm versus 210mm/5.6 = 37.5mm, reducing the aperture towards long focal lengths allows for significantly more compact lens designs. This variation in aperture is avoided in professional movie lenses as a change in the irradiance while zooming is perceived as being disruptive and can subsequently be compensated only at great expense and effort and with losses in quality.

The equation describing the aperture versus magnification was already given earlier in this text:

$$K = \left(1 - \frac{\beta}{\beta_p}\right)\frac{f'}{\varnothing_{EP}}.$$

Unfortunately, the usefulness of this equation is limited: Only in lenses in which overall lens movement is used for focusing do the focal length f′ and the pupil diameter (and thus also the pupil magnification β_p) remain constant for all focus distances and can the aperture be expressed directly as a function of the magnification (given β_p). With a lens system involving focusing of individual lens groups, pupil size and focal length are dependent on the magnification. The right hand side of the above equation does not provide any information as long as $f'(\beta)$, $\beta_p(\beta)$ und $\varnothing_{EP}(\beta)$ are not known from the optical design data. Making the dependencies on magnification explicit, we obtain the following equation for the aperture:

$$K(\beta) = \left(1 - \frac{\beta}{\beta_p(\beta)}\right)\frac{f'(\beta)}{\varnothing_{EP}(\beta)}.$$

With modern professional cinematography lenses, optical designs with overall lens movement focusing are the exception. All lenses of the ARRI/ZEISS Ultra Prime- and Master Prime series use either one or two lens groups within the lens system for focusing.

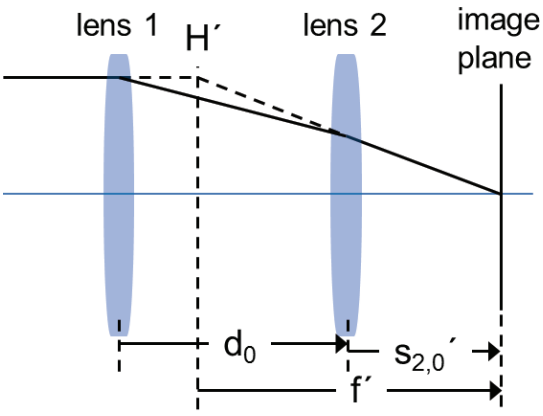

Fig. 20: Notation of distances of the 2-lens system for imaging of object distance infinity.

There are many different implementations for the focusing function in optical design. Before explaining some of them in detail, we consider the simple example of a symmetrical two-lens

system and study the different ways in which the focal length, the pupil sizes and thus the f-number can change depending on the focusing method.

Assume that each of the two lenses has a focal length of $f_1'=f_2'=150$mm. For the object distance "infinity" ($\beta=0$) the lenses are positioned at a distance of d=75mm from each other. Rearranging the equation for the total focal length

$$\frac{1}{f'} = \frac{1}{f_1'} + \frac{1}{f_2'} - \frac{d}{f_1' f_2'}$$

into the form

$$f' = \frac{f_1' f_2'}{f_1' + f_2' - d},$$

we obtain a total focal length of f´=100mm for infinite object distance. The image plane is situated at a distance $s_2'=50$mm from the second lens.

We now consider the following three possibilities to focus on an object located at a finite distance from the lens:

a) Movement of the rear lens L2 (blue graphs)

b) Movement of both lenses L1 and L2 with a constant distance d to each other (red graphs)

c) Movement of the front lens L1 (green graphs)

With the object at infinity, the aperture stop is assumed to be located exactly between the two lenses at a distance of 37.5mm. When focusing, this distance will remain constant relative to the front lens L1 in all three cases. Therefore the position and size of the entrance pupil, i.e. the image of the diaphragm through Lens 1 will also always remain unchanged.

Fig. 21 shows the lens configurations as well as the entrance and exit pupil for these three focusing methods with the magnification values $\beta=0$, -0.1 and -0.2:

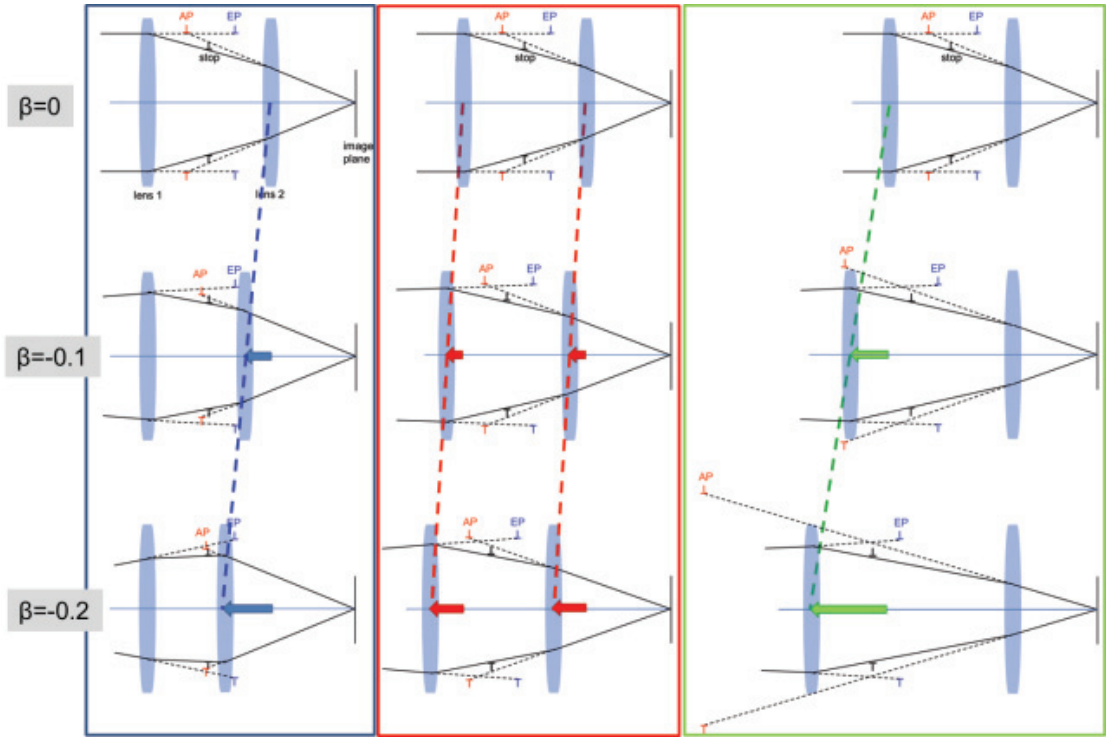

Fig. 21: Lens configuration and pupil positions of the 2-lens system for the magnification values β=0, -0.1 and -0.2.

The relative change in the f-number in comparison to the initial aperture K_0 is distinctly different. In this example, the change in the aperture is greatest when focusing the front lens and smallest when focusing the rear lens:

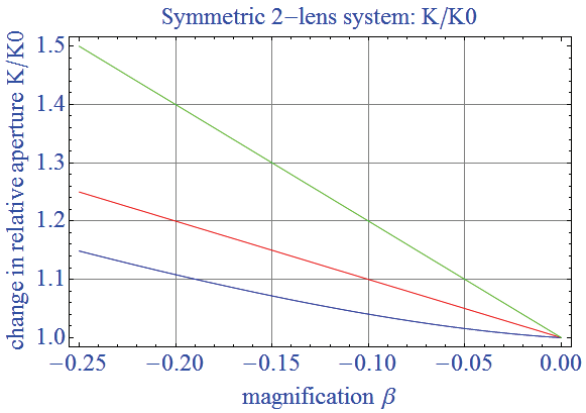

Fig. 22: Relative change in f-number for the 3 focusing methods under consideration.

The tables 1a), b), c) show the lens data for different magnifications. In this context, s_2' represents the distance of the second lens L2 to the image plane, s´ the distance from the exit pupil to the image plane, and L the distance from the object to the image plane. The remaining nomenclature is as given before.

β	K(β)/K0	s'_2	d	s´	β_p	f´	L	$Ø_{EP}$	$Ø_B$	$Ø_{AP}$
0	1	50	75	100	1	100	Infinity	100	62.5	100
-0.05	1.02	58.43	66.57	94.49	0.93	96.39	2106	100	62.5	93.03
-0.1	1.04	65.96	59.04	91.11	0.88	93.38	1115	100	62.5	87.57
-0.15	1.07	72.83	52.17	89.09	0.83	90.79	789	100	62.5	83.13
-0.2	1.11	79.19	45.81	87.99	0.79	88.52	629	100	62.5	79.40
-0.25	1.15	85.13	39.87	87.54	0.76	86.50	534	100	62.5	76.21

Tab. 1a): Focusing with Lens 2 (stop fixed with respect to Lens 1).

β	K(β)/K0	s'_2	d	s´	β_p	f´	L	$Ø_{EP}$	$Ø_B$	$Ø_{AP}$
0	1	50	75	100	1	100	Infinity	100	62.5	100
-0.05	1.05	55	75	105	1	100	2180	100	62.5	100
-0.1	1.1	60	75	110	1	100	1185	100	62.5	100
-0.15	1.15	65	75	115	1	100	857	100	62.5	100
-0.2	1.2	70	75	120	1	100	695	100	62.5	100
-0.25	1.25	75	75	125	1	100	600	100	62.5	100

Tab. 1b): Focusing with overall lens movement.

β	K(β)/K0	s'_2	d	s´	β_p	f´	L	$Ø_{EP}$	$Ø_B$	$Ø_{AP}$
0	1	50	75	100	1	100	Infinity	100	62.5	100
-0.05	1.1	50	86.25	122.22	1.11	105.26	2286	100	62.5	111.11
-0.1	1.2	50	97.50	150.00	1.25	111.11	1298	100	62.5	125.00
-0.15	1.3	50	108.75	185.71	1.43	117.65	975	100	62.5	142.86
-0.2	1.4	50	120.00	233.33	1.67	125.00	820	100	62.5	166.67
-0.25	1.5	50	131.25	300.00	2.00	133.33	731	100	62.5	200.00

Tab. 1c): Focusing with Lens 1 (stop following movement of Lens 1).

The movement of the focusing lens group is smallest with the overall movement method and largest when focusing with the front lens. While all desired focus distances can be achieved with the overall movement and the front lens focusing methods, rear lens focusing is mechanically limited as Lens 2 will abut onto the diaphragm at approximately β=-0.26.

It can also be seen that, at same magnifications, the object image distances L are different for the individual focusing methods. Conversely, this means that two lenses having the same minimum optical distance (MOD) may differ in their respective smallest magnifications, depending on the focusing method.

As a fourth focusing option, it would also be possible to move the two lenses independently from each other, i.e. with a variable distance d. In principle, this results in an infinite number of implementation options. In real lenses, using two lens groups for focusing the movement of one of the groups is defined to be linear and the movement of the second group is adapted accordingly, which usually results in a non-linear moving mechanical shifting group. Real lenses are usually more complex and have additional degrees of freedom, which influence the pupil positions and sizes, the focal length of the system and the dependency of these parameters on the object distance . In contrast to our simple example, the focal lengths of the lenses (or of the lens groups represented by their principal planes) are usually different, and real lenses often consist of more than just two groups.

Even though the number of options seems excessive, the fact that optical designs do have certain typical structures (e.g. in order to obtain the most compact possible lens or meet size specifications for camera construction) allows one to formulate general rules for the functional dependency of aperture variation. This subject will be discussed in the following sections.

F-number vs. magnification when focusing with overall lens movement

Optical designs of the double Gauss type (called "Planar", and earlier "Biotar" at Carl Zeiss – cf. the historical information in the article "Planar" by Hubert Nasse) and also the symmetric wide angle design "Biogon" often use overall movement without variable air spaces for focusing purposes. Most lenses of the ZM series for rangefinder cameras in the 24x36mm² format use overall lens movement. In spite of the high apertures up to K=2, at weights of less than 300g they are very light and compact given this image format.

The heavier SLR camera lenses, in contrast, more frequently use internal focusing. But here, too, "normal" focal lengths, i.e. 50mm, sometimes also 85mm, are often focused with overall lens movement. Fig. 23 shows the ZE/ZF Planar 1.4/85mm when focusing on an object situated at infinity and at close range.

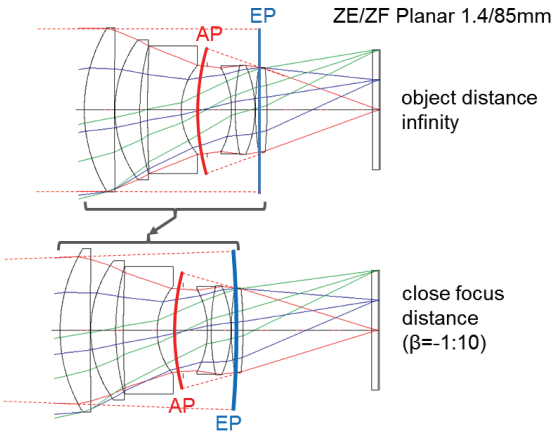

Fig. 23: ZE/ZF Planar 1.4/85mm: Long distance versus close-up focusing.

When focusing with overall lens movement the diaphragm remains at the same distance relative to the rear portion of the lens, therefore the exit pupil (i.e. the image of the diaphragm through the rear lenses in the optical system) retains a constant size. When focusing, the entire lens system, and thus also the exit pupil, is shifted towards the object by the distance

$$\Delta s' = \beta \cdot f' .$$

This follows from the equation $s'=(\beta_p-\beta)\cdot f'$ given before: Accordingly, for β=0 (object distance infinity) the distance of the exit pupil from the image plane is $s_0'=\beta_p\cdot f'$, and the equation $(s_0'-s')=\beta\cdot f'$ for the positional change in the image plane follows.

Thus the f-number rises towards the close range due to the growing distance between the exit pupil and the image plane, while the size of the exit pupil remains constant. This reduction of the maximum image-forming angle, i.e. the increase of the f-number, can directly be deduced from fig. 24 for a single lens (in this case the exit pupil corresponds to the lens).

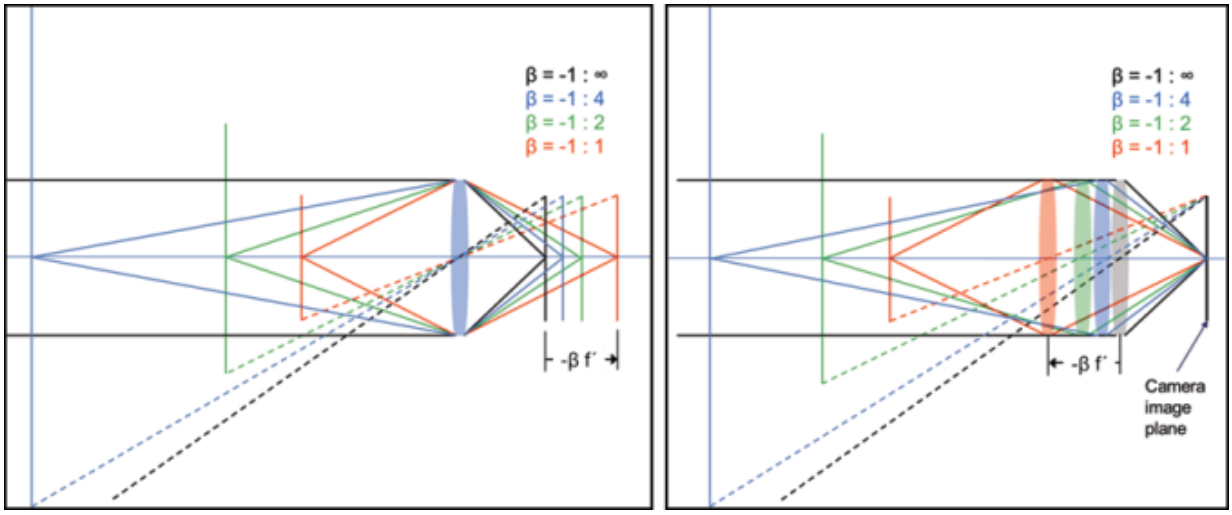

Fig. 24: Focusing with simple lens with fixed lens position (left) or fixed image plane position (right). The angular aperture decreases towards closer object distances.

The ratio of the aperture $K=s'/\varnothing_{AP}$ relative to the initial aperture $K_0=s_0'/\varnothing_{AP}$ is then $K/K_0=s'/s_0'=((\beta_p-\beta)f')/(\beta_p f')$, i.e.

$$\frac{K}{K_0} = 1 - \frac{\beta}{\beta_p}.$$

The pupil magnification β_p always remains the same for all distances as all lenses maintain the same distance from the diaphragm.

The magnification β is a negative number, as photographic lenses yield images that are inverted with respect to the object. (For the sake of simplicity, the minus sign is not included in the distance figures engraved on the focus ring of the lens.) Since β is negative, the factor $1-\beta/\beta_p$ becomes larger for objects situated at a closer distance. Fig. 25 shows the dependency of $1-\beta/\beta_p$ versus β_p for a typical close-range magnification of β=-1:10.

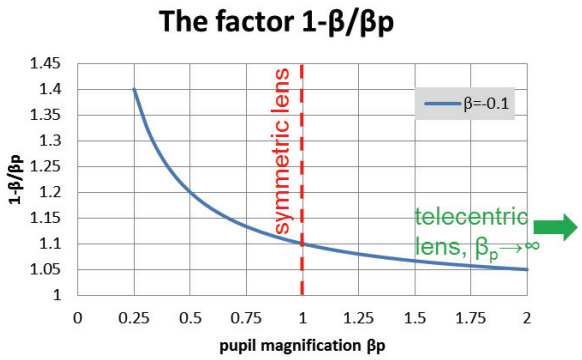

Fig. 25: The relative change of aperture $K/K_0 = 1-\beta/\beta_0$ for overall lens movement focusing versus pupil magnification β_p.

For a symmetrical lens ($\beta_p=1$) the aperture $K=s'/\varnothing_{AP}$ changes by 10% when focusing with lens magnification β=0 vs. β=-1:10. For a telecentric lens ($\beta_p\rightarrow\infty$), i.e. when the exit pupil is at infinity and the chief rays strike the image plane at a 90 degree angle, the aperture does not vary with the distance.

F-number vs. magnification when focusing with movable lens groups

Focusing with individual lens groups, so-called “floating elements”, offers the optical designer further options to improve lens performance (contrast, distortion, etc.) over the distance range and to suppress the “breathing” effect which is undesirable in cinematography. Breathing is a change of the field-of-view depending on the focus distance. The advantage for the mounting technology as compared to overall lens movement consists in lighter movable groups and thus in fast, low noise movements of the focusing lens groups combined with low wear.

Fig. 26 shows the ZE/ZF Macro-Planar 2/100mm. At close range, the exit pupil performs a substantial movement forward and thus appears smaller as seen from the image plane. Hence the f-number increases in the close range. In this optical system, two lens groups are moved in order to achieve a constant imaging quality over the entire distance range up to the magnification of -1:2.

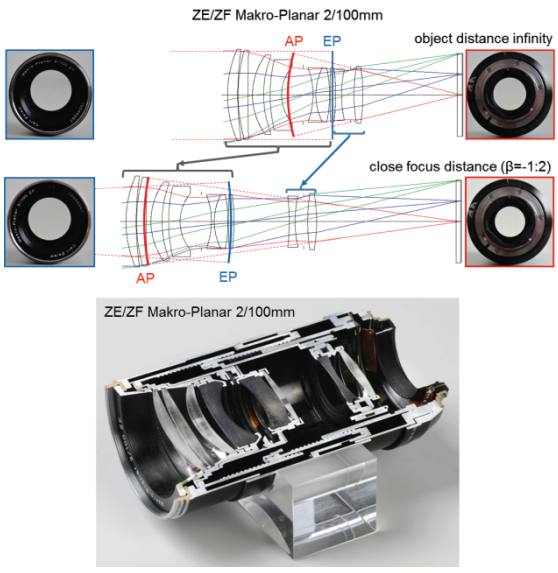

Fig. 26: Focusing mechanism of ZE/ZF Makro-Planar 2/100mm.

The data of the f-numbers as a function of the magnification are given below for the lens series ARRI/ZEISS Ultra Prime and Master Prime as well as for the ZE/ZF series. In each case, the magnification range is represented down to the minimum value of each lens. The change in the irradiance is stated in terms of exposure values.

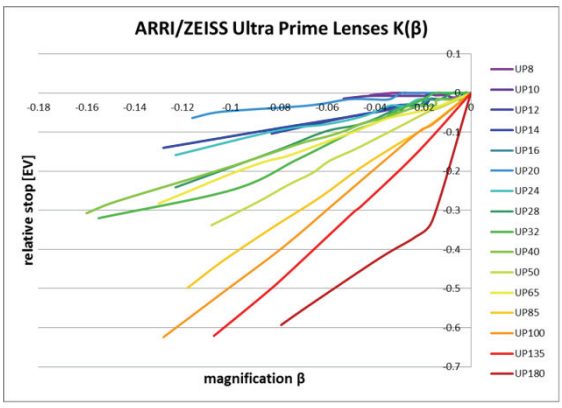

Fig. 27: Change of exposure value versus magnification of ARRI/ZEISS Ultra Prime lenses.

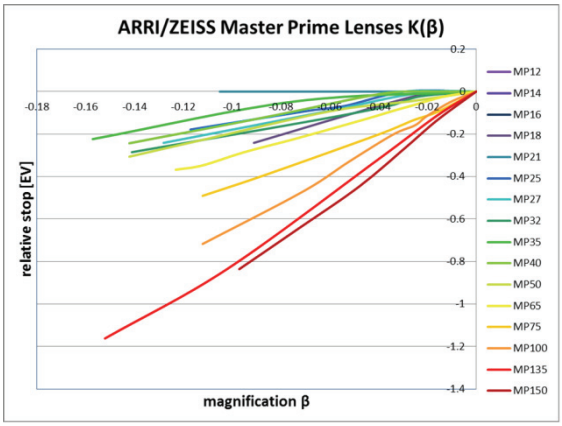

Fig. 28: Change of exposure value versus magnification of ARRI/ZEISS Master Prime lenses.

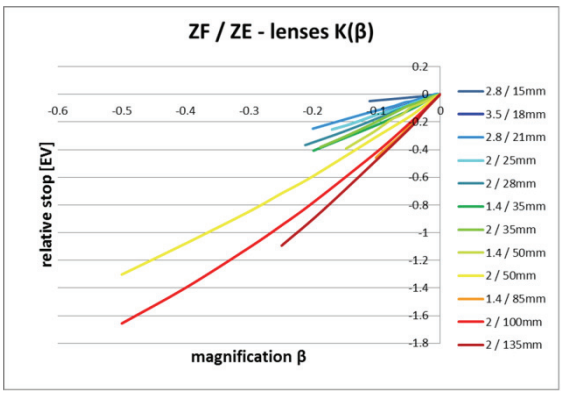

Fig. 29: Change of exposure value versus magnification of the ZE/ZF-lenses.

In all lens series discussed, the change in the f-number is more pronounced for lenses with longer focal lengths. The f-number varies for almost all lenses in a manner that is approximately linear with respect to the magnification. There are generally three factors contributing to the variation of relative apertures: The change in the focal length, the entrance pupil size relative to its value for object distance infinity, and the expression $1-\beta/\beta_p(\beta)$:

$$\frac{K(\beta)}{K_0} = \left(1 - \frac{\beta}{\beta_p(\beta)}\right)\left(\frac{f'(\beta)}{f'_0}\right)\left(\frac{\varnothing_{EP,0}}{\varnothing_{EP}(\beta)}\right).$$

If these three factors are analyzed for the data pertaining to the lenses under consideration, it can be established that the relative aperture change in the ZE/ZF lens series and the ARRI/ZEISS Ultra Prime lenses can be decently approximated by means of

$$\frac{K(\beta)}{K_0} \approx 1 - \frac{\beta}{\beta_p(\beta = 0)}.$$

Therefore, for these lenses, the pupil magnification for object distance infinity essentially determines the change in the f-number. The variation of the f-number K is the smaller, the larger the pupil magnification β_p is. The tables 2, 3 and 4 show an excerpt from these data for lenses with long focal lengths (with the notation $\beta_{p,0}=\beta_p(\beta=0)$).

2/50mm	β	$1-\beta/\beta_{p,0}$	$1-\beta/\beta_p$	$\varnothing_{EP,0}/\varnothing_{EP}$	f'/f'_0	K/K_0
	0.000	1.00	1.00	1.00	1.00	1.00
	-0.025	1.02	1.02	1.00	1.00	1.03
	-0.049	1.04	1.04	1.01	1.00	1.05
	-0.100	1.09	1.09	1.02	1.00	1.11
	-0.201	1.17	1.17	1.03	1.01	1.22
	-0.250	1.21	1.21	1.04	1.01	1.28
	-0.300	1.26	1.25	1.05	1.02	1.33
	-0.400	1.34	1.33	1.06	1.03	1.44
	-0.500	1.43	1.41	1.07	1.04	1.56

1.4/85mm	β	$1-\beta/\beta_{p,0}$	$1-\beta/\beta_p$	$\varnothing_{EP,0}/\varnothing_{EP}$	f'/f'_0	K/K_0
	0.000	1.00	1.00	1.00	1.00	1.00
	-0.025	1.03	1.03	1.01	1.00	1.04
	-0.046	1.06	1.06	1.02	1.00	1.07
	-0.053	1.07	1.07	1.02	1.00	1.09
	-0.063	1.08	1.08	1.02	1.00	1.10
	-0.081	1.10	1.10	1.03	1.00	1.13
	-0.101	1.13	1.13	1.03	1.00	1.17

2/100mm	β	$1-\beta/\beta_{p,0}$	$1-\beta/\beta_p$	$\varnothing_{EP,0}/\varnothing_{EP}$	f'/f'_0	K/K_0
	0.000	1.00	1.00	1.00	1.00	1.00
	-0.025	1.03	1.03	1.01	1.01	1.04
	-0.050	1.05	1.05	1.01	1.01	1.08
	-0.100	1.11	1.11	1.02	1.02	1.15
	-0.200	1.22	1.21	1.04	1.04	1.31
	-0.250	1.27	1.26	1.05	1.05	1.38
	-0.300	1.32	1.31	1.06	1.06	1.46
	-0.400	1.43	1.40	1.07	1.08	1.62
	-0.500	1.54	1.49	1.09	1.10	1.77

2/135mm	β	$1-\beta/\beta_{p,0}$	$1-\beta/\beta_p$	$\varnothing_{EP,0}/\varnothing_{EP}$	f'/f'_0	K/K_0
	0.000	1.00	1.00	1.00	1.00	1.00
	-0.028	1.04	1.04	1.01	1.00	1.05
	-0.047	1.07	1.07	1.01	1.00	1.08
	-0.178	1.27	1.29	1.02	1.01	1.32
	-0.249	1.37	1.41	1.02	1.01	1.45

Tab. 2: Lens data relevant for variation of f-number of some ZE/ZF-lenses.

UP100	β	$1-\beta/\beta_{p,0}$	$1-\beta/\beta_p$	$\varnothing_{EP,0}/\varnothing_{EP}$	f'/f'_0	K/K_0
	0.000	1.00	1.00	1.00	1.00	1.00
	-0.016	1.03	1.03	1.00	1.00	1.03
	-0.021	1.03	1.03	1.01	0.99	1.03
	-0.036	1.06	1.06	1.01	0.99	1.06
	-0.056	1.09	1.09	1.03	0.98	1.10
	-0.078	1.12	1.12	1.04	0.98	1.14
	-0.102	1.16	1.16	1.05	0.97	1.19
	-0.128	1.20	1.20	1.07	0.97	1.24

UP135	β	$1-\beta/\beta_{p,0}$	$1-\beta/\beta_p$	$\varnothing_{EP,0}/\varnothing_{EP}$	f'/f'_0	K/K_0
	0.000	1.00	1.00	1.00	1.00	1.00
	-0.016	1.03	1.03	1.01	0.99	1.04
	-0.028	1.06	1.06	1.02	0.99	1.06
	-0.046	1.10	1.10	1.03	0.98	1.10
	-0.049	1.10	1.10	1.03	0.98	1.11
	-0.076	1.16	1.16	1.04	0.97	1.17
	-0.086	1.18	1.18	1.05	0.96	1.19
	-0.107	1.23	1.22	1.06	0.95	1.23

UP180	β	$1-\beta/\beta_{p,0}$	$1-\beta/\beta_p$	$\varnothing_{EP,0}/\varnothing_{EP}$	f'/f'_0	K/K_0
	0.000	1.00	1.00	1.00	1.00	1.00
	-0.016	1.03	1.03	1.09	0.99	1.12
	-0.023	1.04	1.05	1.09	0.99	1.13
	-0.038	1.07	1.08	1.09	0.98	1.15
	-0.067	1.13	1.14	1.08	0.97	1.20
	-0.079	1.15	1.17	1.08	0.97	1.22

Tab. 3: Lens data relevant for variation of f-number of some ARRI/ZEISS Ultra Prime lenses.

Fig. 30 shows the pupil magnification (at infinite object distance) of the ARRI/ZEISS Ultra Prime and Master Prime lenses versus focal length. It becomes apparent that the pupil magnification is larger for lenses with short focal lengths and that accordingly the f-number variation is less pronounced.

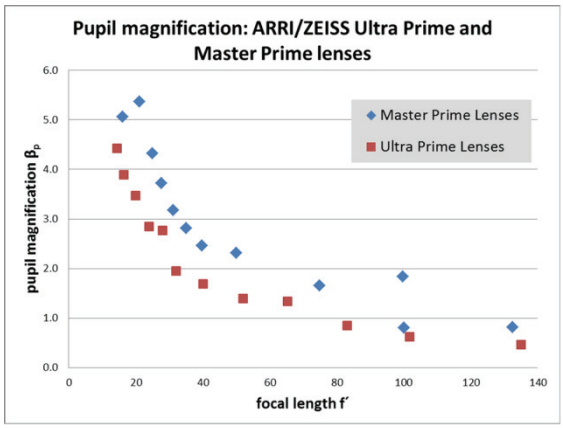

Fig. 30: Pupil magnification of the ARRI/ZEISS Ultra Prime and Master Prime lenses.

The pupil magnification values are somewhat higher for the ARRI/ZEISS Master lenses than for the Ultra Prime lenses of the same focal length, respectively, as the exit pupil is farther away from the image plane. In this way, with the higher aperture of T1.3 as compared to T1.9 it is possible to achieve e.g. the same relative illumination in the corners of the image.

However, the approximation $K(\beta)/K_0 \approx 1-\beta/\beta_{p,0}$ does not apply universally. In the ARRI/ZEISS Master Prime lenses for instance, the aperture changes are mainly due to a relative change of the entrance pupil sizes $\varnothing_{EP}(\beta)/\varnothing_{EP,0}$.

MP 75	β	$1-\beta/\beta_{p,0}$	$1-\beta/\beta_p$	$\varnothing_{EP,0}/\varnothing_{EP}$	f'/f'_0	K/K_0
	0.000	1.00	1.00	1.00	1.00	1.00
	-0.015	1.01	1.01	1.02	0.99	1.03
	-0.026	1.02	1.02	1.04	0.99	1.05
	-0.040	1.02	1.02	1.06	0.99	1.07
	-0.086	1.05	1.05	1.12	0.97	1.14
	-0.112	1.07	1.07	1.15	0.96	1.18

MP 100	β	$1-\beta/\beta_{p,0}$	$1-\beta/\beta_p$	$\varnothing_{EP,0}/\varnothing_{EP}$	f'/f'_0	K/K_0
	0.000	1.00	1.00	1.00	1.00	1.00
	-0.010	1.01	1.01	1.02	1.00	1.02
	-0.020	1.01	1.01	1.04	0.99	1.04
	-0.025	1.01	1.01	1.05	0.99	1.05
	-0.034	1.02	1.02	1.07	0.98	1.07
	-0.052	1.03	1.03	1.12	0.98	1.12
	-0.071	1.04	1.03	1.17	0.97	1.17
	-0.112	1.06	1.05	1.27	0.96	1.28

MP 135	β	$1-\beta/\beta_{p,0}$	$1-\beta/\beta_p$	$\varnothing_{EP,0}/\varnothing_{EP}$	f'/f'_0	K/K_0
	0.000	1.00	1.00	1.00	1.00	1.00
	-0.016	1.02	1.02	1.04	0.98	1.04
	-0.041	1.05	1.05	1.12	0.96	1.12
	-0.102	1.12	1.11	1.32	0.91	1.33
	-0.152	1.19	1.16	1.47	0.87	1.49

MP 150	β	$1-\beta/\beta_{p,0}$	$1-\beta/\beta_p$	$\varnothing_{EP,0}/\varnothing_{EP}$	f'/f'_0	K/K_0
	0.000	1.00	1.00	1.00	1.00	1.00
	-0.016	1.02	1.02	1.05	0.98	1.04
	-0.029	1.03	1.03	1.10	0.96	1.09
	-0.048	1.05	1.05	1.17	0.94	1.16
	-0.072	1.08	1.07	1.26	0.92	1.24
	-0.097	1.10	1.09	1.35	0.90	1.32

Tab. 4: Lens data relevant for variation of f-number of some ARRI/ZEISS Master Prime lenses.

The ARRI/ZEISS Master Prime lenses with focal lengths of 40mm and more are focused by means of the movement of two lens groups in order to provide excellent correction for the breathing phenomenon. To this end a negative lens group is moved towards the fixed positive front group. This causes the refractive power of the lens group before the diaphragm to decrease for the close range. Accordingly the virtual image of the diaphragm, i.e. the entrance pupil, becomes smaller for objects located at a closer distance. In the ARRI/ZEISS Ultra Prime lenses, on the other hand, the refractive power of the front lens group does not change when focusing.

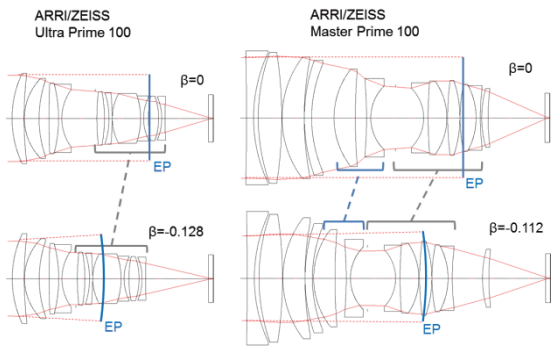

Fig. 31: Focusing mechanisms of the ARRI/ZEISS Ultra Prime 100 and the ARRI/ZEISS Master Prime 100.

The decline of the pupil magnification towards longer focal lengths results from the fact that the entrance pupil becomes larger in lenses with a longer focal length: In fact, when imaging from infinity we have $K_0=f'/\varnothing_{EP}$, i.e. $\varnothing_{EP}=f'/K_0$, according to which with the same aperture (in the ARRI/ZEISS Master Prime lenses $K_0=1.2$ and with the Ultra Prime lenses $K_0=1.9$) the entrance pupil size is directly proportional to the focal length. The size of the exit pupil on the other hand remains approximately equal for all lenses of the same lens series, because the position of the exit pupil remains similar as a result of the relationship $\varnothing_{AP}=s'/K_0$. Accordingly, the maximum chief ray angles in the image plane are similar for all focal lengths. These principles for the size of the exit pupil do, however not hold as strictly as those governing the size of the entrance pupil: They are essentially a consequence of the available space as given by the camera layout. These conditions are determined by the size of the camera bayonet, the necessary distance of the last lens element of the optical system to the image plane (camera with mirror to the optical viewfinder, beam splitter or electronic viewfinder) and the size of the image field. The more limited the given camera construction space, the more similar are the exit pupil positions within a particular lens series.

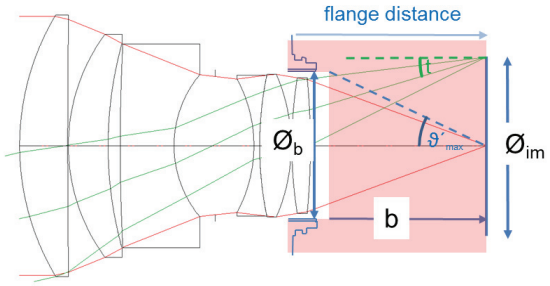

Fig. 32: On constraints due to camera construction space.

In the F-mount of Nikon, for example, the image diagonal is $\varnothing_{im}=\sqrt{24^2+36^2}\,\text{mm}=$ 43.2mm, the minimum distance from the last lens to the image plane is b > 38.4mm, as determined by the camera mirror, and the diameter of the inner ring on the bayonet is $\varnothing_b$ = ca. 36mm (limiting the diameters of the last lens elements; cf. fig. 32). With this geometry, the relative aperture K cannot become smaller than approximately 1.2. The telecentricity of the chief ray must be larger than approximately 14°. This corresponds to a minimum distance of the exit pupil from the image plane of about 85mm. The minimal telecentricity also depends on the vignetting allowed at the edge of the field.

The DigiPrime lenses for cameras with three separate image sensors in 2/3"-format, which are separated via a beam splitter system (cf. fig. 33), are necessarily telecentric on the image side, as a non-telecentricity would result in a relative image shift between the three image planes. The exit pupils lie close to infinity, and the aperture remains constant for any object distance.

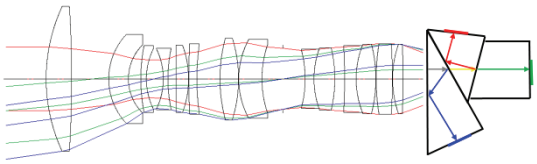

Fig. 33: DigiPrime Distagon T1.6/40mm with camera beam splitter system: the distance between the last lens element and the image sensor planes is greater than 55mm, the optical path length through the glass blocks (refractive index times distance) is more than 82mm.

Construction space constraints are one reason why the optical design of lenses for different camera systems can vary substantially. In the current Zeiss lens program there is a Distagon 2.8/21mm in the ZE/ZF series for SLR cameras, and a Biogon 2.8/21mm in the ZM range finder camera series. In the Biogon, the ratio of exit to entrance pupil size $\beta_p=\varnothing_{AP}/\varnothing_{EP}$ is approximately 1.3, while it is 3 in the Distagon.

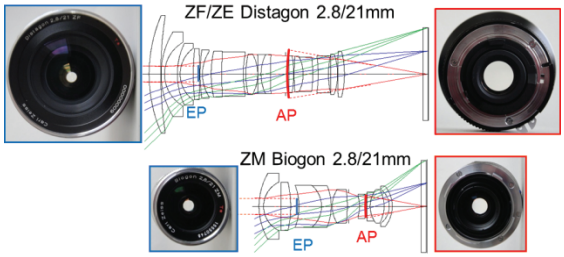

Fig. 34: Entrance and exit pupil of the ZE/ZF Distagon 2.8/21mm and the ZM Biogon 2.8/21mm.

The Biogon and Distagon lens types have the following general characteristics:

Biogon:

- (quasi) symmetrical design
- negative menisci outside, therefore smaller, relaxed ray angles inside the lens system
- asymmetrical aberration types (distortion, coma, lateral chromatic aberration) can easily be corrected because of the symmetrical design
- the distance between the last lens and the image plane must be small
- large angles of incidence onto the image plane
- natural vignetting due to the incidence angle t (telecentricity) according to $\cos^4 t$ remains when stopping down.

Distagon:

- retrofocus type: In front, an overall negative power and in the rear a positive power lens group

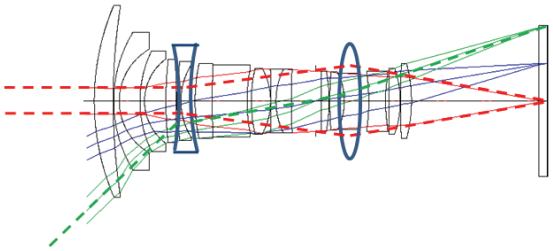

Fig. 35: Retrofocus lens type (ZE/ZF Distagon 2.8/21mm).

- allows for greater distance between the last lens and the image plane
- as a rule, at high apertures construction space constraint causes loss of brightness towards the edge due to vignetting; vignetting decreases when the lens is stopped down.

The table 5 summarizes a number of data for the Biogon 2.8/21mm ZM and Distagon 2.8/21mm ZE/ZF. The variable w denotes the maximum semi-diagonal object-side field-of-view angle, and t the telecentricity in the corner of the image field.

	w_{ob} [°]	$\varnothing_{EP}$ [mm]	$\varnothing_{AP}$ [mm]	β_p	s´ [mm]	t [°]	$\cos^4(t)$
Biogon 2.8/21mm ZM	45.2	7.5	10.1	1.3	28.3	37.4	0.4
Distagon 2.8/21mm ZE/ZF	45.2	7.5	22.6	3	64.3	18.6	0.81

Tab. 5: Some lens data of ZE/ZF Distagon 2.8/21mm and ZM Biogon 2.8/21mm.

The apertures and focal lengths, and thus also the size of the entrance pupil are equal in both cases, namely $\varnothing_{EP} = f'/K_0 = 21mm/2.8 = 7.5mm$. In the Biogon, because of the symmetrical layout, the angles of the chief ray in the image space are similar in magnitude to those in the object space (approx. 46° at a focal length of 21mm). Thus the exit pupil closely approaches the image plane. This facilitates a highly compact optical design, however, at the cost of natural vignetting. This $\cos^4 t$-brightness decline due to the large telecentricity angle t also remains when the lens is stopped down. In digital cameras, the larger angles of incidence sometimes bring about color shading and crosstalk between the color channels of the sensor mosaic (e.g. with Bayer pattern).

Within a certain scope, these errors can be compensated by means of image processing in the camera or a shift of the microlenses that are located directly in front of the sensor. In the ever more frequently employed backside illuminated sensors these errors are significantly reduced, as the light directly impinges on the light sensitive silicon crystal and need not pass any area past conductor paths between color filter and photo diodes.

Because of the greater distance to the image plane, the retrofocus type (Distagon) on the

other hand has a greater distance between the exit pupil and the image plane and thus also a larger exit pupil ($\varnothing_{AP}=s'/K_0$). For this reason, the pupil magnification $\beta_p=\varnothing_{AP}/\varnothing_{EP}$ is larger with the Distagon than with the Biogon.

Hubert Nasse exhaustively described these lens types in his article about "Distagon, Biogon, and Hologon".

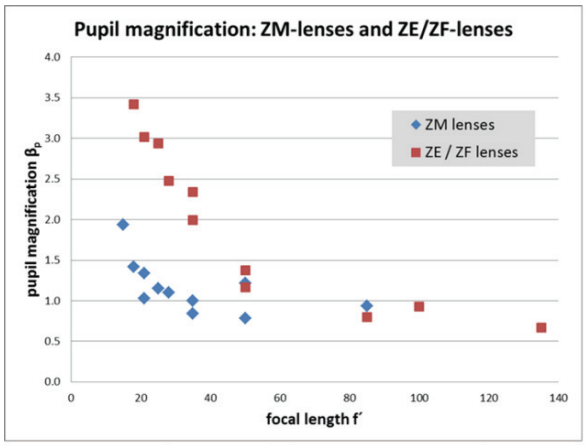

ZM lenses	β_p
Distagon 2.8/15mm	1.94
Distagon 4/18mm	1.42
Biogon 2.8/21mm	1.34
Biogon 4.5/21mm	1.03
Biogon 2.8/25mm	1.15
Biogon 2.8/28mm	1.10
Biogon 2/35mm	1.00
Biogon 2.8/35mm	0.85
Sonnar 1.5/50mm	0.78
Planar 1.2/50mm	1.08
Planar 2/50mm	1.22
Tele-Tessar 4/85mm	0.93

ZE/ZF lenses	β_p
Distagon 2.8/15mm	7.12
Distagon 3.5/18mm	3.42
Distagon 2.8/21mm	3.02
Distagon 2/25mm	2.93
Distagon 2/28mm	2.47
Distagon 1.4/35mm	2.34
Distagon 2/35mm	1.99
Planar 1.4/50mm	1.38
Makro-Planar 2/50mm	1.17
Planar 1.4/85mm	0.80
Makro-Planar 2/100mm	0.93
Apo Sonnar 2/135mm	0.67

Fig. 36: Pupil magnification of ZM and ZE/ZF-lenses.

In the wide angle lenses of the ZM series with very small focal lengths there are deviations from the symmetry and a transition from the Biogon to the Distagon design, as a minimum distance of 15mm between the last lens and the image plane is respected. In this way, the ZM lenses for range finder cameras remain compatible with through-the-lens (TTL) exposure measurement. Since at approximately 39mm this minimum distance between the last lens and the image plane is much larger in SLR cameras, there are larger deviations in the wide angle SLR lenses from symmetrical lens design and thus distinctly higher values of the pupil magnification.

Until now, our discussion has concentrated on the behavior of the f-number variation over distance at maximum aperture. But how does the f-number change in relation to the initial aperture when stopping down? If the f-number changes, by e.g. one exposure value at close range and with full aperture, will it also change by one exposure value if the lens is stopped down?

The answer is: Essentially, the dependency $K(\beta)/K_0$ on magnification remains unchanged for any initial aperture K_0. This is understandable, as this dependency can be described by means of the paraxial lens data. This is shown in fig. 37 using the example of the ARRI/ZEISS Master Macro 100 and of the ZE/ZF Macro-Planar T* 2/100mm.

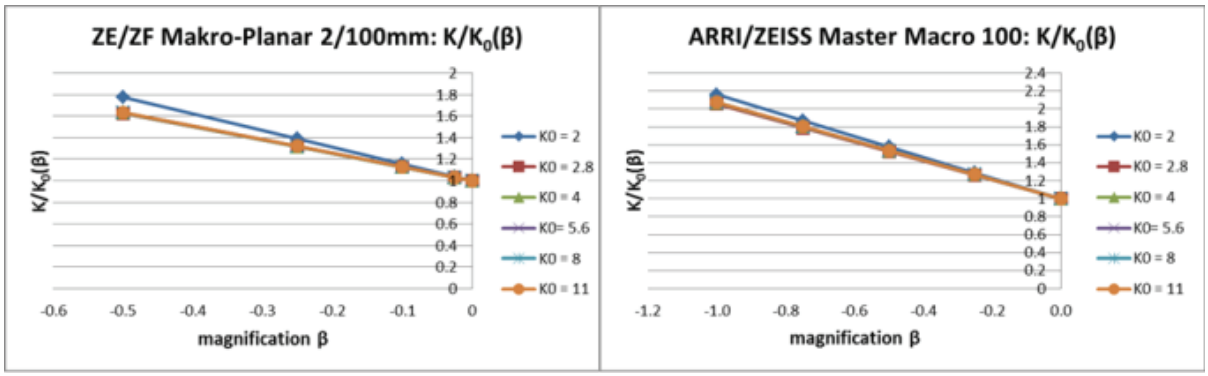

Fig. 37: Relative change in the aperture K/K_0 versus magnification with different initial apertures K_0 for the ARRI/ZEISS Master Macro 100 (left) and the ZE/ZF Macro Planar 2/100mm.

The slight deviations at maximum aperture result from the fact that it is not the iris diaphragm that limits the path of rays, but a diaphragm positioned further back in the system that principally has the function to curtail the light at the edge of the field in a defined manner.

We have seen that in all examples given until now the f-numbers increase towards the close range. Accordingly, with macro lenses (typically having maximal magnifications of -1:2 or -1:1) more significant changes can be expected in the apertures than with standard lenses (with maximal magnifications of -1:20 to approx. -1:10, as "close-up lens" approx. -1:7 to -1:4). On the other hand, the aperture variation in turn depends on the optical design. This can be exemplified by comparing two macro lenses whose apertures distinctly differ as they approach the close range (cf. fig. 38).

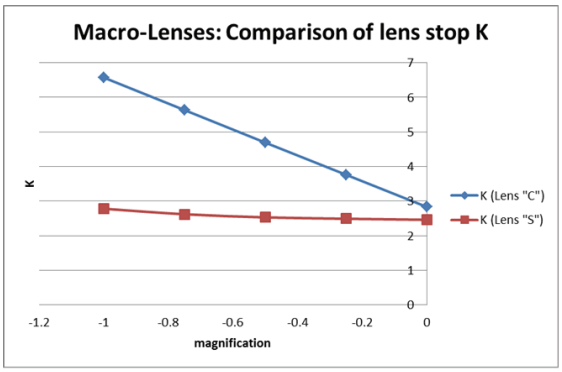

Fig. 38: f-number vs. magnification of two macro lenses „S" und „C".

We name these two macro lenses "S" and "C":

"S": Jae-myung Ryu et. al. USP 2011/00996410 (data scaled, so that the focal length is 100mm as in "C")

"C": Contax Macro Planar 2.8/100mm for small format 36x24mm2 film

They have similar field of views and initial apertures and are illustrated in fig. 39 for β = 0 and β = -1:1. The build of the two lenses is distinctly different: "S" consists of five groups: The first, third, and fifth are fixed, so that the length of the lens remains constant when focusing. Towards the close range area, the second (front negative) and the fourth (rear positive) focus groups are moved towards each other and towards the center of the lens sys-

tem. “C” consists of two groups, both of which are moved forward when focusing; the front group moves faster than the rear group.

“S”:

β	β_p	f´ [mm]	$Ø_{EP}$ [mm]	$Ø_{AP}$ [mm]	s´ [mm]	K
0	1.28	100.19	41.47	53.13	128.34	2.42
-0.25	0.99	92.84	48.56	48.28	115.51	2.39
-0.5	0.68	89.62	64.11	43.63	105.80	2.42
-0.75	0.43	83.75	92.03	39.52	98.78	2.50
-1	0.28	73.64	124.91	35.06	94.31	2.69

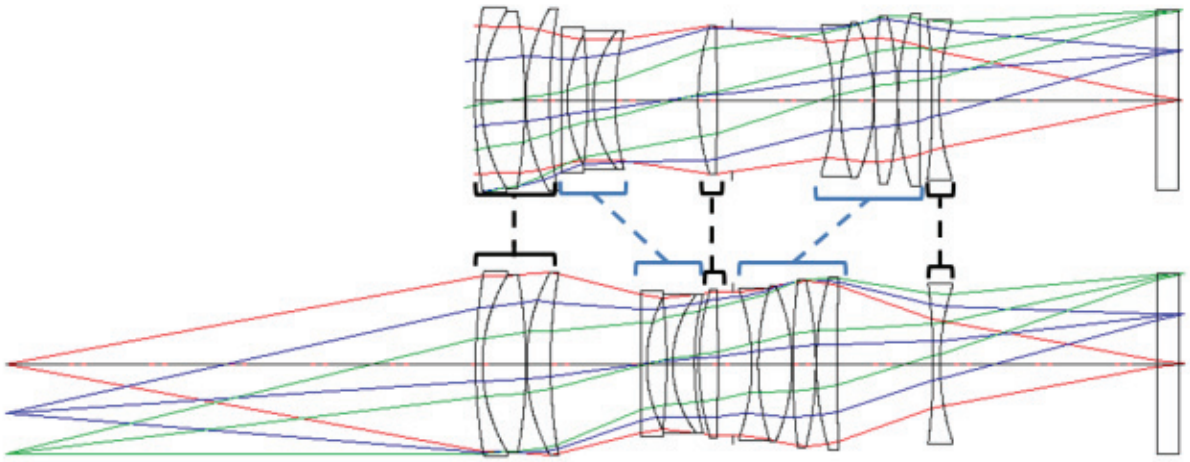

“C”:

β	β_p	f´ [mm]	$Ø_{EP}$ [mm]	$Ø_{AP}$ [mm]	s´ [mm]	K
0	0.77	100.19	35.36	27.33	77.44	2.83
-0.25	0.74	94.59	35.72	26.26	93.18	3.55
-0.5	0.70	89.73	35.96	25.28	107.94	4.27
-0.75	0.67	85.46	36.14	24.39	121.77	4.99
-1	0.65	81.67	36.27	23.58	134.77	5.72

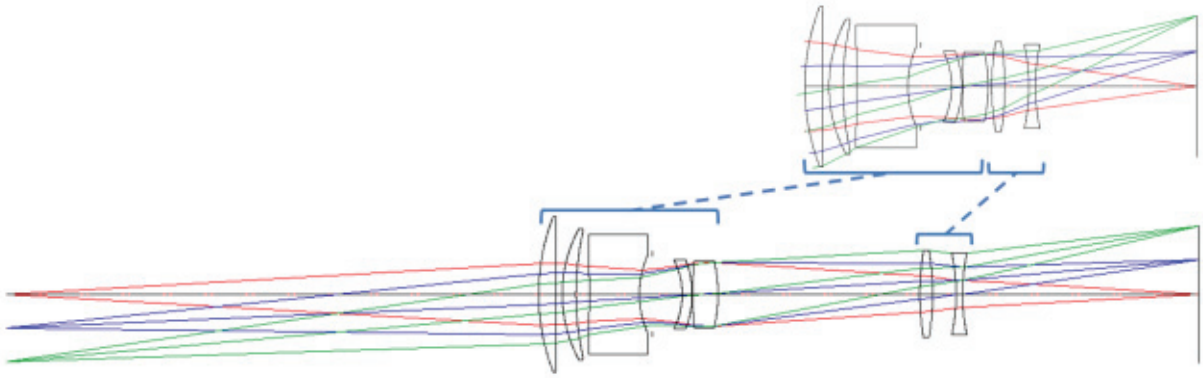

Fig. 39: Focusing mechanism and lens data of the macro lenses „S“ und „C“.

In “S” the f-number remains almost at the initial value over the entire distance range, while “C” decreases by more than 2 f-stops. Especially because of the strong change in the pupil sizes and the pupil magnification over the distance range, in “S” all factors in

$$\frac{K(\beta)}{K_0} = \left(1 - \frac{\beta}{\beta_p(\beta)}\right)\left(\frac{f'(\beta)}{f'_0}\right)\left(\frac{\varnothing_{EP,0}}{\varnothing_{EP}(\beta)}\right)$$

substantially contribute to the relative change in aperture (cf. table 6).

β	$1-\beta/\beta_{p,0}$	$1-\beta/\beta_p$	$\varnothing_{EP,0}/\varnothing_{EP}$	f'/f'_0	K/K_0
0	1.00	1.00	1.00	1.00	1.00
-0.25	1.20	1.25	0.85	0.93	0.99
-0.5	1.39	1.73	0.65	0.89	1.00
-0.75	1.59	2.75	0.45	0.84	1.03
-1	1.78	4.56	0.33	0.74	1.11

Tab. 6: Lens data relevant for change in f-number of “S”.

In “C”, in contrast, the dominant factor is $1-\beta/\beta_p$ (cf. table 7).

β	$1-\beta/\beta_{p,0}$	$1-\beta/\beta_p$	$\varnothing_{EP,0}/\varnothing_{EP}$	f'/f'_0	K/K_0
0	1.00	1.00	1.00	1.00	1.00
-0.25	1.32	1.34	0.99	0.94	1.25
-0.5	1.65	1.71	0.98	0.90	1.51
-0.75	1.97	2.11	0.98	0.85	1.76
-1	2.29	2.54	0.97	0.82	2.02

Tab. 7: Lens data relevant for change in f-number of “C”.

With similar imaging performance, the lens “C” is substantially smaller and lighter as well as shorter in the normal distance range.

The practical benefits of a constant aperture is however very limited in macro lenses: for a magnification of -1:2 with an aperture of f/2.8, the depth of field range is distinctly less than 1mm. Even the maximum aperture of f/6.5 available in the lens “C” in the extreme close range will in practice seldom be used. Even with a “still object“ and a tripod because of the extremely small depth of field range, rather further reducing the lens aperture.

References

Abbe, E. (1873). *Beiträge zur Theorie des Mikroskops und der mikroskopischen Wahrnehmung*, [Contributions to Microscope Theory and Microscopy Perception] Archive for microscopic anatomy, Vol. 9, Issue 1, p. 413-418.

Abbe, E. (1879). *Ueber die Bedingungen des Aplanatismus der Linsensysteme* [On the condition of aplanatism of lens systems]. Ernst Abbe, Gesammelte Abhandlungen I, chapter 11, Georg Olms Verlag.

Berek, M. (1930). *Grundlagen der praktischen Optik. Analyse und Synthese optischer Systeme* [Principles of Practical Optics, Analysis and Synthesis of Optical Systems], de Gruyter, Berlin. (The reprint (1970) was abridged by omitting Chapter 10 "*Energiebilanzen*" [Energy balances].)

Clausius, R. (1887). *Die Mechanische Wärmetheorie* [The Mechanical Theory of Heat], 3. Edition, Printing and Publication by Friedrich Vieweg und Sohn; §12 and §14.

Conrady, A. E. (1905). *The Optical Sine Condition*, Monthly Notices of the Royal Astronomical Society, Vol. 65, p. 501-509.

Czapski, S. (1904). *Grundzüge der Theorie der optischen Instrumente nach Abbe* [Principles of the Theory of Optical Instruments According to Abbe], published by Otto Eppenstein, Johann Ambrosius Barth, Leipzig.

Flügge, J. (1955). *Das Photographische Objektiv* [The Photographic Lens], Springer-Verlag Vienna.

Goodman, D. S. (1993). *The F-word in optics*, Optics and Photonics News, 38-39.

Hofmann, C. (1973), *Die Abbesche Sinusbedingung von 1873 und ihre Weiterentwicklung in den vergangenen 100 Jahren* [Abbe's Sine Condition of 1873 and its Further Development in the Past 100 Years] Feingerätetechnik [Precision Instrument Technology], Vol. 22., No. 4, p. 151-159.

Jae-myung Ryu, Seongnam-si, USP 2011/00996410 A1, April 28th 2011, *Macro Lens System and Pickup Device including the same*.

Kingslake, R. (1978). *Lens Design Fundamentals*, Academic Press.

Kingslake, R. (1989). *A History of the Photographic Lens*, Academic Press.

Mansuripur, M. (1998), *Abbe´s Sine Condition*, Optics and Photonics News, Vol. 9, Issue 2, pp. 56-60; also as Chapter 1 in: Mansuripur, M. (2009), *Classical Optics and its Applications*, 2nd ed., Cambridge.

Merté, W. (1932). *Bauarten der Photographischen Objektive* [Design of Photographic Lenses] in: *Handbuch der wissenschaftlichen und angewandten Photographie* [Handbook of Scientific and Applied Photography] *Band 1:* [Vol. 1]: *Das Photographische Objektiv* [The Photographic Lens], Julius Springer Publishing House, Vienna.

Nasse, H. H. (2011). *Planar*, Carl Zeiss Camera Lens News 40.
http://blogs.zeiss.com/photo/en/wpcontent/uploads/2011/07/en_CLB_40_Nasse_Lens_Names_Planar.pdf

Nasse, H. H. (2011). *Distagon, Biogon und Hologon*, Carl Zeiss Camera Lens News 41.
http://blogs.zeiss.com/photo/en/wpcontent/uploads/2011/12/en_CLB41_Nasse_LensNames_Distagon.pdf

Schmutzer, E. (1989). *Grundlagen der Theoretischen Physik* [Principles of Theoretical Physics], *Band 1* [Volume 1], BJ-Wissenschaftsverlag, Mannheim, Vienna, Zurich.

Smith, W. J. (2008). *Modern Optical Engineering*, 4th edition, McGraw-Hill.

Wandersleb, E. (1952). *Die Lichtverteilung im Grossen in der Brennebene des photographischen Objektivs* [Light Distribution in the Focal Plane of a Photographic Lens] in Akademie-Verlag Berlin.

Weizel, W. (1949). *Lehrbuch der Theoretischen Physik* [Textbook of Theoretical Physics], *Band 1* [Vol. 1], Springer-Verlag.

Carl Zeiss AG
Camera Lenses
73446 Oberkochen
Germany

www.zeiss.com/photo